Electrical and magnetotransport properties of Nd-based manganite nanoparticles

C. Krishnamoorthy, K. Sethupathi, V. Sankaranarayanan, R. Nirmala, and S. K. Malik

Citation: Journal of Applied Physics **99**, 08Q310 (2006); doi: 10.1063/1.2167350
View online: http://dx.doi.org/10.1063/1.2167350
View Table of Contents: http://scitation.aip.org/content/aip/journal/jap/99/8?ver=pdfcov
Published by the AIP Publishing

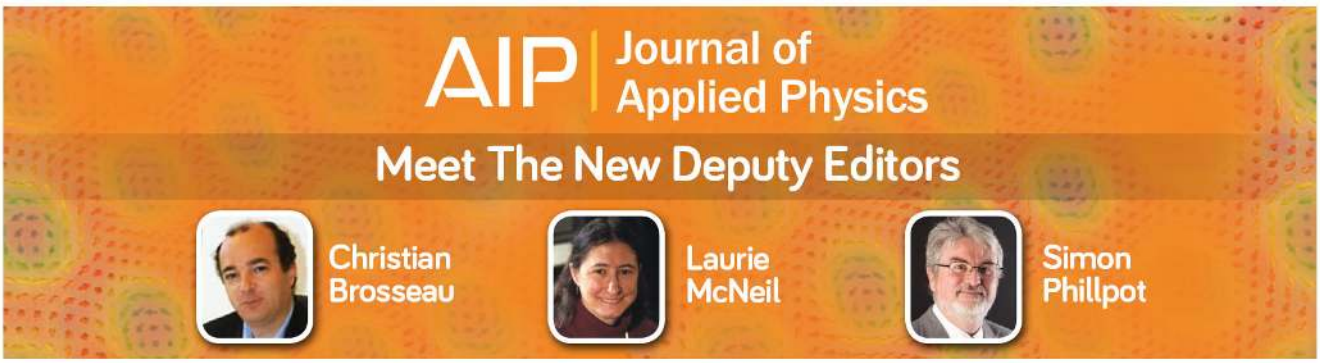

Electrical and magnetotransport properties of Nd-based manganite nanoparticles

C. Krishnamoorthy,[a] K. Sethupathi,[b] and V. Sankaranarayanan
Department of Physics, Indian Institute of Technology Madras, Chennai 600 036, India

R. Nirmala and S. K. Malik
Tata Institute of Fundamental Research, Mumbai-400 005, India

(Presented on 2 November 2005; published online 20 April 2006)

Electrical and magnetotransport properties of nanocrystalline $Nd_{0.7}Sr_{0.3}MnO_3$ sample having an average particle size of 45 nm have been studied. The resistivity in paramagnetic regime follows Mott's variable range hopping mechanism with an average hopping distance of about 21 Å. The observed magnetoresistivity (MR) has best been described by assuming that canted spins and defects are distributed all over the volume of the nanoparticle. The MR could be quantitatively best fitted to spin-dependent hopping model, together with phase-separation phenomenon. In this model, hopping barrier is proportional to the angle between the magnetic moments of the clusters. The hopping barrier height is minimum when the moments are parallel to each other and is maximum when the moments are randomly oriented. The fit yields a small cluster size of about two to three lattice constant dimensions in the paramagnetic (PM) phase and of about four to five lattice constants in the ferromagnetic (FM) phase. The results indicate that FM phase contributes to MR at low fields, whereas PM phase contributes at relatively high fields. © *2006 American Institute of Physics*. [DOI: 10.1063/1.2167350]

I. INTRODUCTION

Recently hole-doped perovskite manganites have attracted considerable attention due to their colossal magnetoresistance (CMR). The CMR properties of manganites can be quantitatively well understood by taking into account the magnetic phase separation (PS), in addition to the qualitative double exchange mechanism (DEM).[1] It has been now established that these intrinsically phase-separated regions have dimensions from nanometer[2] to micrometer[3] in percolative and fractal-like form. Mayr *et al.*[4] have shown that the percolation both in nanometer as well as in micrometer phases yields indeed similar results of resistivity.

The CMR manganites with relatively small grain sizes exhibit pronounced magnetoresistivity (MR) under a low applied magnetic field and/or over a wide temperature range.[5] The electronic and magnetic properties of nanocrystalline materials are modified due to the influence of structural and magnetic disorder at the interior and grain boundaries. Néel[6] attributed the increase of magnetic susceptibility (χ) in NiO antiferromagnetic (AFM) nanoparticles to the possibility of some canted spins and random concentration of vacancies at the interior. Coey[7] accounted the decrease in saturation magnetization (M_s) of γ-Fe_2O_3 ferrimagnetic nanoparticles to the existence of noncollinear spins, but not disordered, at the surface of the nanoparticles. He also reported the nonexistence of nonmagnetic layer at the surface of the nanoparticles. However, he could not exclude the possibility of some canted spins and random vacancies at the interior of the nanoparticles. Parker *et al.*[8] have shown that the canted spins are distributed all over the volume of the γ-Fe_2O_3 nanoparticles and are due to finite-size effect.

In order to understand the effect of reduction of grain size, prepared at relatively low temperatures, in CMR manganites we have chosen optimally doped $Nd_{0.7}Sr_{0.3}MnO_3$.

II. EXPERIMENT

Nanocrystalline $Nd_{0.7}Sr_{0.3}MnO_3$ sample was prepared from stoichiometric amount of high-purity Nd_2O_3, $SrCO_3$, $Mn(CH_3COO)_2.4H_2O$, and $C_6H_8O_7.H_2O$ by citrate complex method. Nd_2O_3 and $SrCO_3$ have been converted to their respective nitrates by dissolving them in dilute HNO_3. All the metal solutions were added to citric acid solution. The resultant solution was evaporated at 80–90 °C for several hours. The obtained precursor was calcined at 800 °C for 3 h to make nanoparticles. The phase purity and crystal structure of the sample were studied by x-ray diffraction (Shimadzu XD-D1). The morphology of the sample was determined by transmission electron microscopy (Phillips). ac magnetic susceptibility was measured using physical properties measuring system (PPMS) (Quantum Design). To measure electrical resistivity, the pressed pellet was sintered for 10 min in a preheated furnace, at calcination temperature, and then quenched to room temperature to enable connectivity between the particles and to avoid further grain growth. The transverse MR was measured using PPMS.

III. RESULTS AND DISCUSSIONS

The x-ray-diffraction (XRD) profile of the calcined sample shows a broad distribution due to nanocrystalline character. The obtained diffraction profile was best fitted to orthorhombic perovskite structure of space group Pnma. Fig-

[a]Electronic mail: kris.phy@gmail.com
[b]Author to whom correspondence should be addressed; electronic mail: ksethu@iitm.ac.in

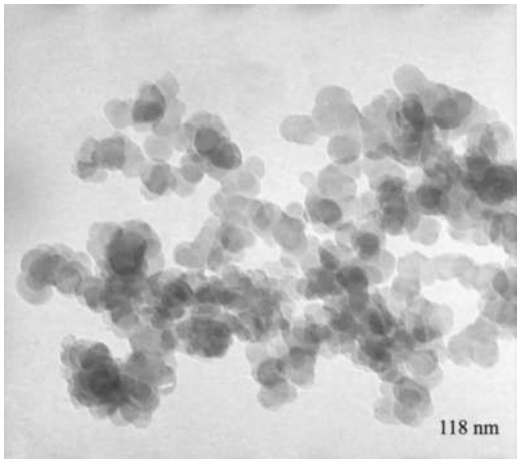

FIG. 1. TEM micrograph of the $Nd_{0.7}Sr_{0.3}MnO_3$.

ure 1 shows the transmission electron microscopy (TEM) micrograph of the sample. It shows that the particles are nearly spherical in shape and are narrowly distributed. The estimated average particle size was found to be 45 nm. Around 7% of Mn ions lie in the surface layer of the nanoparticle. ac susceptibility of the sample as a function of temperature shows a paramagnetic (PM)-to-ferromagnetic (FM)-like transition (T_C) at around 135 K (not shown here). The sample shows a broad magnetic transition. Such a broad transition is indicative of the coexistence of both short- and long-range orderings of ferromagnetic clusters. The electron magnetic resonance (EMR) studies show the coexistence of FM and PM phases below 290 K.[9]

Upon cooling the sample, resistivity smoothly increases and shows a broad insulator-metal transition (hump) at 137 K. The observed resistivity, in the PM region, could be best fitted to Mott's variable range hopping (VRH) model (Fig. 2). The fit yields 3.5 Å, 21 Å, and 0.1 eV for the localization length, average hopping distance, and hopping energy, respectively. These values are reasonable in view of the VRH model.

The magnetoresistivity is defined as

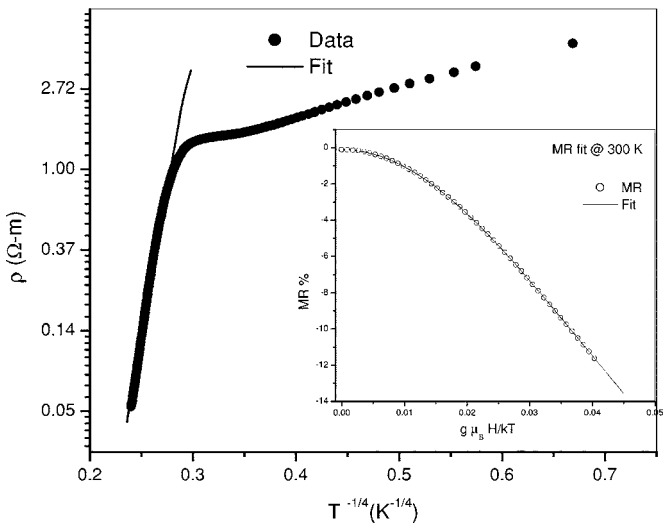

FIG. 2. ln (ρ) as a function of $T^{-1/4}$. The fit yields a good fit over paramagnetic regime. The inset shows MR as a function of $x(=g\mu_B H/k_B T)$ at 300 K. The solid line shows the fit to the data.

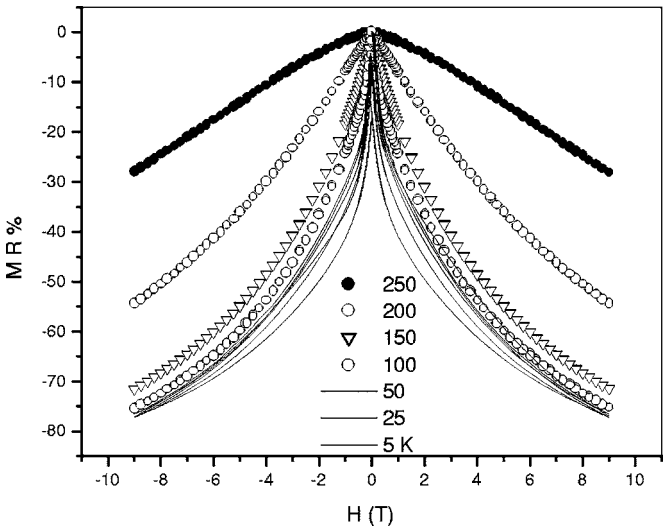

FIG. 3. MR as a function of an applied magnetic field H.

$$\text{MR}\,\% = \frac{\rho(H,T) - \rho(0,T)}{\rho(0,T)} \times 100, \tag{1}$$

where $\rho(H,T)$ is the resistivity in the presence of the applied magnetic field H at temperature T and $\rho(0,T)$ is the resistivity in the absence of H.

Figure 3 shows the MR as a function of up to 9 T and down to 5 K. The MR loops show no butterfly feature at low fields (LF) in the FM regime. Rather they show hysteresis up to 9 T which may be due to spin memory effect and/or increase of metallic phases upon application of H. It is also noted that the MR curves are nonlinear at high fields ($H > 0.5$ T). This suggests that the sample is not behaving like a typical granular FM metal dispersed in nonmagnetic (SiO_2) matrix, in which the MR(H) shows a butterfly feature at low fields and then saturates with no hysteresis above few hundreds of millitesla field.[10] The butterfly feature has been explained by spin-polarized tunneling (SPT) mechanism. The field-dependent MR has also been observed in bulk polycrystalline manganites in the FM region and has been explained qualitatively by SPT model.[11] Hwang *et al.*[11] reported that the low-field ($\leqslant 0.5$ T) MR increases upon cooling the sample. It is also reported that the MR changes ~68%, of the total MR at 5 T and 5 K, at low fields ($\leqslant 0.5$ T) and ~32% at the high-field region (>0.5 T). However, in the present sample MR is around 16% at 100 K and remains at ~20% down to 5 K. It indicates that the low-field MR is weakly temperature dependent below T_C. Moreover, the MR changes ~27%, of the total MR at 9 T and 5 K, up to 0.5 T and ~73% above 0.5 T. This suggest that SPT may not be the dominant transport mechanism in our sample. It has also been reported that the sharp increase of MR(H) at low fields is due to the alignment of intergrain magnetic moments (domains), and the almost linear increase of MR at high fields is due to the alignment of canted spins at intragrains. This suggests that the change in MR in our sample is mainly due to the alignment of canted spins at the intragrain since large changes in MR occur at high fields.

The EMR study of the sample shows phase-separated behavior below 290 K. The resistivity follows hopping

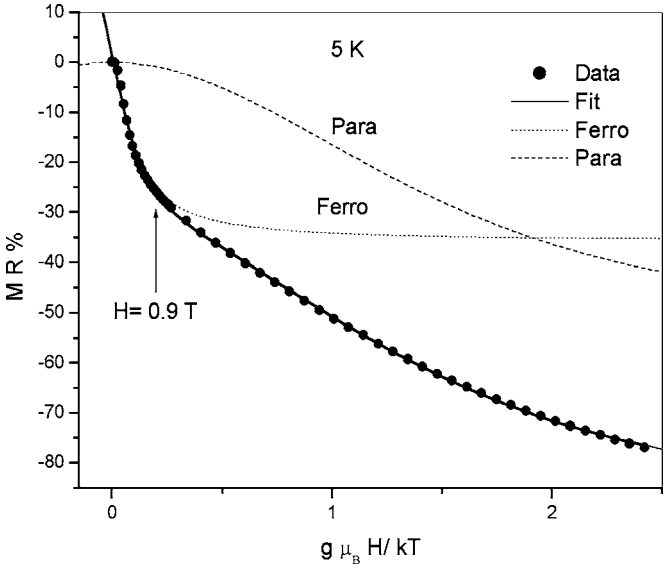

FIG. 4. The fit of MR as a function of $x(=g\mu_B H/k_B T)$ at 5 K. The figure shows para- and ferromagnetic contributions separately.

mechanism among the localized clusters. The canted spins and random vacancies are distributed all over the volume of the nanoparticle.[8] MR shows predominant intragrain canted spin contribution. From the above results, we can infer that the electrons are localized within fractal-like phase-separated regions due to spin-dependent potential resulting from noncollinear spins and random vacancies distributed all over the volume of nanoparticles. The electron transfer between these localized states may be due to hopping or tunneling. In spin-dependent hopping mechanism, the hopping barrier is minimum when the magnetic moments of the hopping sites are parallel and is maximum when the moments are randomly aligned. The magnetic moments of the localized clusters are randomly oriented in the PM phase and are narrowly oriented in the FM phase due to internal molecular field.[12] Assuming spin-dependent hopping between these localized spin clusters, we have fitted the isothermal MR(H) curves to the following expressions:[13]

$$\mathrm{MR}(H,T) = A(T)\mathcal{B}^2(\mu_B g J(T) H/k_B T) \quad \text{in PM phase}, \tag{2}$$

$$\mathrm{MR}(H,T) = D(T)\mathcal{B}(\mu_B g J(T) H/k_B T) \quad \text{in FM phase}, \tag{3}$$

where $\mathcal{B}(\mu_B g J(T) H/k_B T)$ is the Brillouin function, $A(T)$ and $D(T)$ are temperature-dependent prefactors and are proportional to respective components of MR, $g=2$ is Lande's g factor, $J(T)$ is the average spin moment at the hopping site, and H is the applied magnetic field. Here A, D, and J are the fitting parameters. This model assumes hopping conduction both in FM as well as in PM phases, as explained by Wagner *et al.*[13]

At 300 K, the MR(H) is well fitted to single-PM-phase equation (inset of Fig. 2). At $T \leqslant 250$ K, the best fits were obtained to the coexistence of both PM and FM phases. Figure 4 shows the typical fitted MR curve as a function of x ($=g\mu_B H/k_B T$; here H is a variable) at 5 K, with para- and ferromagnetic contributions separately. All MR curves have been fitted similarly. Upon application of the magnetic field, the narrowly oriented spin clusters in the FM regions will align parallel to each other at low fields and thereby increasing the electron hopping. Hence the decrease in resistivity gives rise to an increase of negative MR. Upon further increasing the applied magnetic field, all the spin clusters in the FM regions will completely align and then no further decrease in resistivity will be observed. This leads to the saturation of the MR of the FM component (Fig. 4). Randomly oriented spin clusters in the PM region will align at relatively high fields, resulting in a further decrease of resistivity at high fields. The corresponding increase in MR could be observed at relatively high fields. The MR of the PM component is not saturated even at 9 T magnetic fields. It appears that the randomness of spin clusters is more in the PM phase and/or the conversion of insulating phases into metallic one is not completed even at 9 T and 5 K. The spin cluster size (J) in the PM phase is small and varies between two and three lattice parameters, as reported for other manganites. In the FM component, the cluster size varies between four and five lattice parameters which are almost double the cluster size in PM phase, as expected.

The FM contribution (D), to the total MR, increases from 0% at 300 K to ~42% at 5 K upon cooling the sample. The PM contribution (A) decreases from 100% at 300 K to ~58% at 5 K upon cooling the sample.

IV. CONCLUSIONS

Nanocrystalline $Nd_{0.7}Sr_{0.3}MnO_3$ sample with an average particle size of 45 nm has been prepared by citrate complex method. The magnetoresistivity (MR) has been analyzed by spin-dependent hopping together with phase-separation phenomenon. The results show that (i) the average spin cluster size in the ferromagnetic (FM) phase is about twice that in paramagnetic (PM) phases. The results also indicate that the FM phase contributes to the total MR at low fields and the PM phase contributes at relatively high fields.

[1] E. Dagotto, *Nanoscale Phase Separation and Colossal Magnetoresistance: The Physics of Manganites and Related Compounds* (Springer-Verlag, Berlin, 2003).
[2] A. Moreo, M. Mayr, A. Feiguin, S. Yunoki, and E. Dogatto, Phys. Rev. Lett. **84**, 5568 (2000).
[3] M. Uehara, S. Mori, C. H. Chen, and S.-W. Cheong, Nature (London) **399**, 560 (1999).
[4] M. Mayr, A. Moreo, J. A. Vergés, J. Arispe, A. Feiguin, and E. Dagotto, Phys. Rev. Lett. **86**, 135 (2001).
[5] M. A. Lopez-Quentela, L. E. Hueso, J. Rivas, and F. Ravidulla, Nanotechnology **14**, 212 (2003).
[6] L. Néel, J. Phys. Soc. Jpn. **17**, 676 (1962).
[7] J. M. D. Coey, Phys. Rev. Lett. **27**, 1140 (1971).
[8] F. T. Parker, M. W. Foster, D. T. Margulies, and A. E. Berkowitz, Phys. Rev. B **47**, 7885 (1993).
[9] C. Krishnamoorthy, K. Sethupathi, V. Sankaranarayanan, R. Nirmala, and S. K. Malik (unpublished).
[10] J. Q. Xiao, J. S. Jiang, and C. L. Chein, Phys. Rev. Lett. **68**, 3749 (1992).
[11] H. Y. Hwang, S. W. Cheong, N. P. Ong, and B. Batlogg, Phys. Rev. Lett. **77**, 2041 (1996).
[12] M. Viret, L. Rano, and J. M. D. Coey, Phys. Rev. B **55**, 8067 (1997).
[13] P. Wagner, I. Gordon, L. Trappeniers, J. Vanacken, F. Herlach, V. V. Moshchalkov, and Y. Bruynseraede, Phys. Rev. Lett. **81**, 3980 (1998).